Computer modeling of micropile systems with ZSoil

Andrzej Truty[1]
Aleksander Urbański[2]

Abstract

Complex and simplified FE modeling of micropile-structure static interaction is discussed in the paper. A simplified model in which micropile is represented as a beam embedded in the 3D continuum, through the special frictional Coulomb's interface, is presented. Comparizon of results obtained using simplified and a fully discretized 3D model are shown. Both approaches rely on effective stress principle and therefore effective parameters have to be used.

1. Introduction

A general approach to model soil-structure interaction problems in which micropiles/nails/piles are used to strengthen weak subsoil is presented in the paper. The approach and foregoing applications are implemented and analyzed in ZSoil code designed for solving geotechnical static/dynamic, geometrically linear/nonlinear (large displacements and rotations), problems [ZSOIL 2013].

Certain levels of complexity of a given problem can be analyzed using ZSoil. The general 3D analysis in which both micropile and subsoil are discretized with aid of continuum elements can be replaced by a simplified method where micropile is represented by a typical beam member embedded in the 3D continuum. The latter approach is very powerful from designer point of view because FE model of the structure and subsoil remains unchanged during whole micropile design procedure. Significant reduction of size of the computational model, resulting reduction of CPU time and reduction of hardware resources are beneficial when simplified method is used. For very complex problems this approach can be treated as a first design step to optimize the micropile system that can finally be verified on real 3D continuum model of subsoil and micropiles. Within ZSoil code special Coulomb type interface elements were worked out and implemented to model strong tangential movement of a micropile with respect to the adjacent subsoil. As micropiles may be in contact with several soil layers, each interface element, along the micropile, may inherit strength and stiffness properties of the adjacent soil layer. Strength properties in the interface are defined through user defined multipliers to the tangent of effective friction angle $\tan(\phi')$ and effective cohesion c' of a given soil layer. It has to be mentioned that the proposed FE approach adopts the effective stress principle by Bishop (for fully/partially saturated soils) as most of the enhanced soil models are formulated in terms of effective stresses. Moreover the micropile beam can also be analyzed in materially nonlinear mode, by taking into account complex cross section composition, as well as geometrically

[1] dr hab. inż., profesor nadzwyczajny Politechniki Krakowskiej, e-mail: andrzej.truty@gmail.com

[2] dr hab. inż., profesor nadzwyczajny Politechniki Krakowskiej, e-mail: aurbansk123@gmail.com

nonlinear mode by considering large deflections. These aspects are important in global analysis of safety.

After the introduction the paper consists of three sections in which simplified method of modeling micropiles as beam members embedded in 3D continuum is described first, then short discussion on constitutive modeling aspects for subsoil is given and in the last section practical examples of micropile system modeling are presented.

2. Simplified numerical modeling of micropiles and nails

In order to analyze large computational 3D models of soil-structure interaction, with many micropiles/piles or nails, a simplified discretization methods are needed to reduce computational effort. The goal of the method shown here is to represent micropile/pile/nail as a beam member embedded in the 3D continuum without any mesh conformity restriction. The analyzed discrete system micropile-subsoil-structure is shown in figure 2.1. It consists of a pile discretized with aid of beam finite elements, foundation raft represented here as a shell (plate) element, subsoil discretized with 3D continuum elements, and two, Coulomb type (or purely adhesive), interfaces connecting micropile skin and its tip with subsoil. In case of micropiles skin interface is governed by the Coulomb's friction law while for nails purely adhesive one is used. Interface in the tip of micropile is needed mainly to cancel displacement continuity in case of pull-out forces. The latter effect can be achieved using nonlinear hinge element that can be assumed at the pile tip.

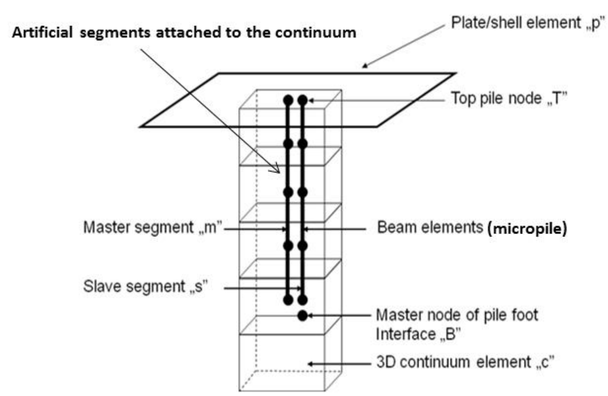

Fig.2.1. Numerical model of a micropile-subsoil-structure system

Three major problems must be solved to allow such an approach i.e. satisfying kinematic continuity of all or selected set of degrees of freedom (DOFs) of nodal point of a given finite element embedded in any other finite element (of the same or different class) and a skin/tip contact interfaces treatment.

As far as general kinematic continuity condition is concerned (for instance connection of a micropile and plate) it is obvious that only common DOFs of a node and given finite element can be unified (for instance nodal point of beam element can be connected to 3D continuum only through translational DOFs, same beam node can be connected to shell element via translational and/or rotational DOFs). The analytical expression of the kinematic continuity condition can be written as follows

$$\mathbf{u}_T = \sum_{i=1}^{Nen} N_i\left(\boldsymbol{\xi}_T\right)\mathbf{u}_i^p \tag{2.1}$$

In the above expression number of nodes in element *p*, to which given nodal point *T* is attached, is denoted by *Nen,* vector of local coordinates of point *T* in element *p* by $\boldsymbol{\xi}_T$, standard interpolation functions by N_i, while vector of displacements in i-th node of element *p* by $\mathbf{u}_i^p$.

In order to fulfill condition (2.1) local coordinates of point *T* must be found first. If dimension Ndm_{LOC} of local element coordinate system (for 3D continuum element Ndm_{LOC}=3, for shell element Ndm_{LOC}=2, for beam/truss element Ndm_{LOC}=1) is equal to the dimension Ndm_{GLO} of global coordinates one (in 3D Ndm_{GLO}=3) vector $\boldsymbol{\xi}_T$ is obtained by solving the following nonlinear set of equations (of size Ndm_{GLO}= Ndm_{LOC})

$$\mathbf{x}_T - \sum_{i=1}^{Nen} N_i\left(\boldsymbol{\xi}_T\right)\mathbf{x}_i^p = \mathbf{0} \tag{2.2}$$

In the remaining cases ($Ndm_{GLO} \neq Ndm_{LOC}$) vector $\boldsymbol{\xi}_T$ is found by minimizing distance of point *T* from element *p*. This functional can be written as follows

$$\left(\frac{\partial\left(\mathbf{x}_T - \sum_{i=1}^{Nen} N_i\left(\boldsymbol{\xi}_T\right)\mathbf{x}_i^p\right)}{\partial\boldsymbol{\xi}}\right)^{\mathrm{T}}\left(\mathbf{x}_T - \sum_{i=1}^{Nen} N_i\left(\boldsymbol{\xi}_T\right)\mathbf{x}_i^p\right) = \mathbf{0} \tag{2.3}$$

In the proposed approach kinematic continuity condition expressed by (2.1) is satisfied by means of method of reduction of dependent DOFs rather than penalty one. Although the method allows to connect nonconforming meshes certain restrictions must be preserved to avoid stress/force oscillations or false interface behavior. To avoid these pathological effects mesh density used to discretize beam members embedded in the 3D continuum has to be approximately the same as the one in the 3D continuum mesh.
All details concerning FE implementation of method of dependent DOFs can be found in [Truty et al 2009].

Another important aspect is related to modeling contact interface behavior on micropile skin and its tip. As it is shown in the figure 2.1 the skin interface is reduced to a line in 3D and therefore it is practically impossible to model gap opening between micropile skin and subsoil. This effect can be important for laterally loaded micropiles. Other potential deficiences, and possible remedies, will be discussed later on.
The contact skin interface is modeled using segment-to-segment approach. Local coordinate system in the interface is shown in figure 2.2.

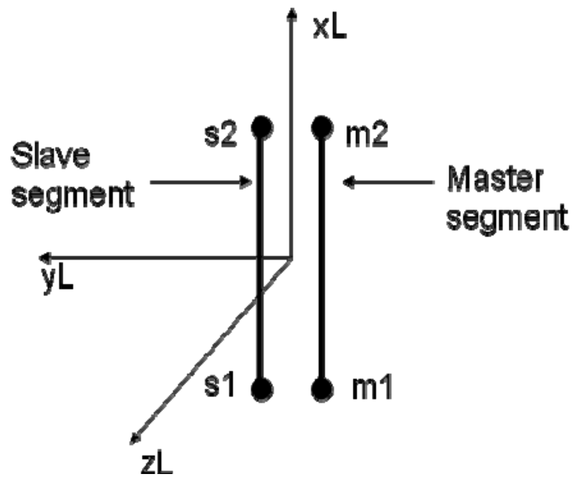

Fig.2.2. Skin interface

The shear stress-generalized shear strain relation at any time instance can be written as follows

$$\tau_{N+1} = \tau_N + k_s\, \Delta\gamma_{N+1} \tag{2.4}$$

where shear stresses an time instances t_n and t_{n+1} are denoted by τ_N, τ_{N+1} , generalized shear strain (understood as a relative tangential displacement) increment by $\Delta\gamma_{N+1}$ and shear penalty factor by k_s. As the interface in our approach is quasi-rigid plastic the k_s parameter should be infinitely large. However, iterative procedures can converge only up to certain value of the shear stiffness. Therefore its value is estimated automatically by the code by assessing current shear elastic stiffness of the adjacent subsoil.

The shear stress must satisfy Coulomb's friction law

$$\| \tau_{N+1} \| \le \sigma_n^{'} \tan(\phi) + c \tag{2.5}$$

while increment of generalized shear strain $\Delta\gamma_{N+1}$ is computed as (here upper indices *m* and *s* are used to distinguish between master and slave segments)

$$\Delta\gamma_{N+1} = \mathbf{e}_{xL}{}^{\mathrm{T}} (\Delta\mathbf{u}_{N+1}^{s} - \Delta\mathbf{u}_{N+1}^{m}) \tag{2.6}$$

The major difficulty in this approach is related to the recovery technique of the effective normal stress in the skin interface. As the interface geometry is reduced to the line in 3D we cannot extract $\sigma_n^{'}$ directly from the interface element. Therefore another simplified procedure was proposed (see Figure 2.3) in which averaged value of $\sigma_n^{'}$ is computed as follows

$$\sigma_n^{'} = \frac{\int_0^{2\pi} \min(\sigma_n^{'}(\theta), 0)\ R\,\mathrm{d}\theta}{2\pi R} \tag{2.7}$$

and integration is performed in 16 points positioned at distance *R* from the micropile axis. To compute $\sigma_n^{'}(\theta)$ superconvergent patch recovery technique is used first [Zienkiewicz et. al 1989] and then radial stress is obtained by standard stress transformation in cylindrical system designed by the micropile axis and given integration point (located at the artificial skin interface) (see Figure 2.3).

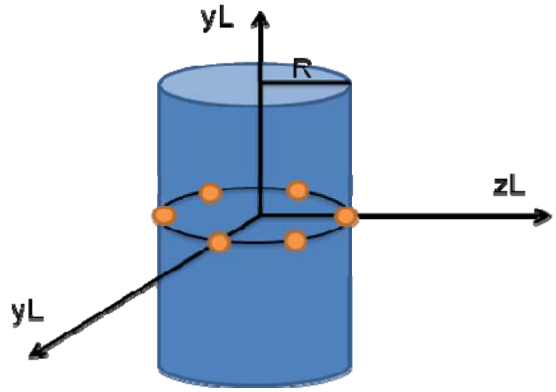

Fig.2.3. Scheme for evaluation of averaged normal stress in the interface

The weakest point in this approach is related to the need of adding extra stress increment (with respect to the geostatic state) to the subsoil, caused by installation of a micropile. This extra stress increment can be deduced for instance from a simplified cavity expansion analysis run as an auxiliary axisymmetric problem with preexisting geostatic initial effective stresses treated as an initial condition, in which the inner surface of cavity is loaded by the pressure value being equal to the vertical effective geostatic stress multiplied by the assumed *K* parameter. A comprehensive study on that can be found in the report by Satibi et al. [7]. One has to mention that such an analysis may yield too crude stress change estimate and can still be far from the reality. Hence load tests carried out on micropile (if are available) should be used to assess value of this *K* parameter. Another crude method to handle that problem is basing on estimation of equivalent friction coefficient and cohesion in the interface that take into account an effect of micropile installation. Last aspect of the interface behavior is related to the effect of dilatancy. This effect is missing so far in our approach but possibilities to include that definitely exist.

The corresponding nodal forces in i-th node of the interface element are computed as follows

$$
\begin{aligned}
f_{xLi} &= \frac{1}{2}\, L\, \boldsymbol{\tau}^{i}_{N+1}\, 2\pi\, R \\
f_{yLi} &= \frac{1}{2}\, L\, \boldsymbol{\sigma}_{\mathbf{yL}}{}^{i}_{N+1} \\
f_{zLi} &= \frac{1}{2}\, L\, \boldsymbol{\sigma}_{\mathbf{zL}}{}^{i}_{N+1}
\end{aligned}
\tag{2.8}
$$

where interface length is denoted by *L* and remaining stress and generalized strains are defined as below

$$\boldsymbol{\sigma}_{\mathbf{yL}}{}^{i}_{N+1} = k_n\, \varepsilon^{i}_{yL} \tag{2.9}$$

$$\boldsymbol{\sigma}_{\mathbf{zL}}{}^{i}_{N+1} = k_n\, \varepsilon^{i}_{zL} \tag{2.10}$$

$$\varepsilon_{yL\,N+1} = \mathbf{e}_{yL}{}^{\mathrm{T}} \left(\mathbf{u}^{s}_{N+1} - \mathbf{u}^{m}_{N+1} \right) \tag{2.11}$$

$$\varepsilon_{zL\,N+1} = \mathbf{e}_{zL}{}^{\mathrm{T}} \left(\mathbf{u}^{s}_{N+1} - \mathbf{u}^{m}_{N+1} \right) \tag{2.12}$$

In the above expressions k_n and k_s are penalty parameters estimated based on elastic properties of the adjacent continuum elements. The k_n is a penalty parameter that preserves continuity of displacements between micropile and subsoil in the plane perpendicular to the micropile axis. Its value is automatically estimated based on current elastic modulus in adjacent to the micropile (at a given point) continuum element. Notion of k_s penalty parameter was discussed earlier.

Another interface that can be activated in this approach is the one at the tip of micropile. The major goal in applying this interface is to allow to model pull-out tests but also to put limits on the maximum stress transferred through the tip. The later effect can frequently be caused by coarse meshes in the continuum near the tip. The only stress/force component exerted on subsoil through the tip is the vertical (normal) one. Values of these quantities are computed as follows

$$f_{xL} = \sigma_{n\,N+1}\ \pi\ R^2 \tag{2.13}$$

$$\sigma_{n\,N+1} = k_n\ \varepsilon_{n\,N+1} \tag{2.14}$$

$$\varepsilon_{n\,N+1} = \mathbf{e}_{xL}{}^{\mathrm{T}} \left(\mathbf{u}^{s}_{N+1} - \mathbf{u}^{m}_{N+1} \right) \tag{2.15}$$

The normal stress under the tip is limited to the user defined value

$$\sigma_{n\,N+1} \le q_c \tag{2.16}$$

where q_c is the assumed maximum normal stress to be transferred by the micropile tip.

In several cases the latter interface may help to reproduce properly force transfer through the skin friction (or adhesion) and tip resistance.

As it was already mentioned this approach is simplified and therefore in bending dominated cases results can be strongly mesh dependent. This is so because the interface is reduced from the 3D surface to the 3D line. To retain mesh objectivity continuum elements adjacent to the beam member should not be smaller than 50-100% of pile/micropile diameter. For axially loaded piles/micropiles this approach yields very accurate results (see TRUTY 2009)

3. Constitutive modeling of subsoil

One of the major sources of mismatch between numerical predictions and measurements is caused by too crude representation of soil behavior in numerical models. In most cases users try to use simple elasto-plastic Mohr-Coulomb model in which elastic stiffness is represented by Young modulus *E.* Such a model is good enough for limit state analyses for soils (bearing capacity or stability) but it frequently fails in practical soil-structure interaction problems and verifying serviceability limit states in general. This fact, led several analysts to strange (obviously not objective) tricks in contact interface treatment when M-C model was used. Since last few years in our daily practice we can make use of more advanced model, the Hardening Soil/Hardening Soil-small (HS/HS-s), that was found to be robust in many soil-structure interaction problems. A comprehensive review of the model, worked out methods for its calibration, examples of applications can be found in [Obrzud et al 2010]. This report is available after installing full/student or demo version of ZSoil software (www.zsoil.com). All theoretical details of the model can be found in PhD thesis by Benz

[Benz 2006]. To summarize this model it is worth to mention that it quite nicely reproduces stiffness changes due to stress and strain variation. Among the other ones of the most important aspect in that model is proper representation of stiffness in a wide range of strains starting from very small to large ones.

4. ZSoil simulations of vertically loaded micro-piles using HS-s model

Prediction of the ultimate and serviceability limit states of the micro-pile foundation system (D=0.2m) - is the aim of the considered example. In the prediction HS-s model is used and its parameters are back analyzed based on results of pile load - tests carried out for three CFA piles from group constructed in the neighborhood. These piles (diameter D=0.6m) were constructed with the regular grid 1.9 x 2.0 m and no foundation raft was built at time the case was investigated. Therefore - the first task was to calibrate parameters of HS-s model for soils using results of pile load tests and soil parameters (c_u, ϕ_u, γ, E_0, M_0) obtained from standard laboratory procedures. Next, the estimated HS-s model parameters were used for analysis of the aforementioned micro-pile system.

4.1 Geotechnical data and estimation of HS-s model parameters

In the considered location, the most important soil layers are marked as IIc (medium dense and dense gravely sands) and III (hard Miocene clays). The two top layers (sands IIa and IIb) are of less importance. The draft for back-analyzed pile is given in Table 4.1.

<table>
<tr><td>Draft</td><td>Geotechnical data</td></tr>
<tr><td rowspan="4">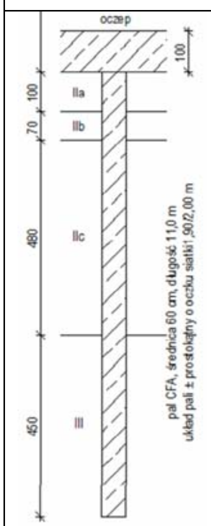
</td><td>IIa – medium dense silty sands I_D = 0,55 ρ_n = 1,80 g/cm3
c_u = 0,0 kPa ϕ_u = 30,5°, E_0 = 51.000 kPa, M_0 = 68.000 kPa</td></tr>
<tr><td>IIb – medium dense medium sands I_D = 0,55 ρ = 1,85/2,00 g/cm3
c_u = 0,0 kPa ϕ =33,5°, E_0 = 87.000 kPa, M_0 = 103.000 kPa</td></tr>
<tr><td>IIc – medium dense and dense gravely sands I_D = 0,60,
ρ_n = 2,00/2,10 g/cm3
c_u = 0,0 kPa, ϕ_u = 39,5°,
E_0 = 155.000 kPa, M_0 = 174.000 kPa</td></tr>
<tr><td>III – Miocene clays
I_L = 0,05, ρ_n = 2,05 g/cm3,
c_u = 57,0 kPa, ϕ_u = 12,0°,
E_0 = 19.500 kPa, M_0 = 34.500 kPa</td></tr>
</table>

Table. 4.1 Geotechnical data

Initial guess of stiffness parameters (all in [kPa]) was worked out based on recommendations given in report [Obrzud 2010 et al], with: $E_{ref,50}$= E_0, E_{oed}=M_0 in geotechnical data. Variable stiffness in HS-S-s model requires also to specify: $E_{ref,ur}$=$E_{ref,50}$*3.0 (unloading-reloading reference stiffness modulus) then initial stiffness modulus (at very small strains): $E_{ref,0}$=$E_{ref,50}$*16.7 (for cohesive soils) and $E_{ref,0}$ = $E_{ref,50}$*3.8 (for sands). Stiffness exponent *m*[-] was set by back-analysis of the case, to get the best fit of measured and computed load-displacement curves in the considered load range (aprox. 1000kN).

The parameters sets IIc and h6 III were finally chosen to represent soils of layer IIc and III in the whole area. Also, dilatancy angle ψ was specified for both class of soils in HS-s material model. These data were used in assessment of foundation system consisting of two groups 3x3 and 3x5 of micro-piles, D=0.20m, connected by a foundation beam, as shown in Fig.4.1.

Another important issue is to model properly the interface betwen the pile and subsoil. Parameters of those were set basing on Polish pile foundation design standard (PN-83-B-02482) for layers IIa,b,c: cv=0kPa , $tg\mu$=1.0; for layer III: cv=50kPa, $tg\mu$=0.

	Eref,ur	Eref,0	Eref,50	Eoed	c[kPa]	m[-]	ψ[o]
II c	**465000**	**596750**	**155000**	**174000**	**0.1**	**0.625**	**10**
h6 III	**58500**	**325605**	**19500**	**34500**	**57**	**0.625**	**3**
h7 III	58500	325605	19500	34500	28	0.625	3
h8 III	58500	325605	19500	34500	57	0.4	3
h9 III	58500	325605	19500	34500	57	0.7	3

Table. 4.2 HS-s stiffness model data

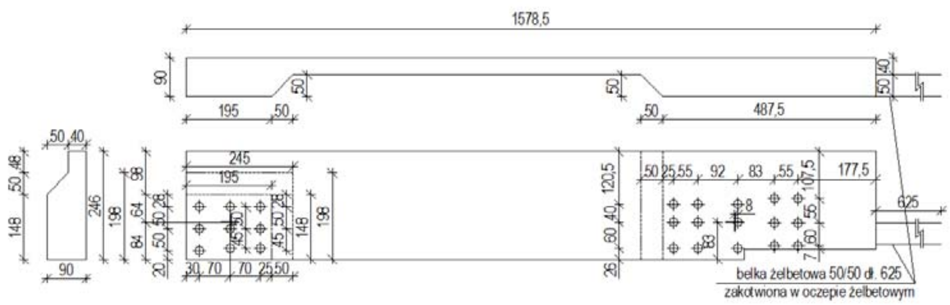

Fig. 4.1 Micro-pile foundation system

4.2 Results of simulations

Some of the results of simulation concerning a single pile (D=0.60m), made with use of the method named as Continuous Flight Auger (CFA), placed within 1.9x2.0m periodic cell, are presented. Reference load was taken as P=1000kN, simulated displacement were approximately u=2mm for different data sets, remaining within dispersion of test result for different piles at the site.

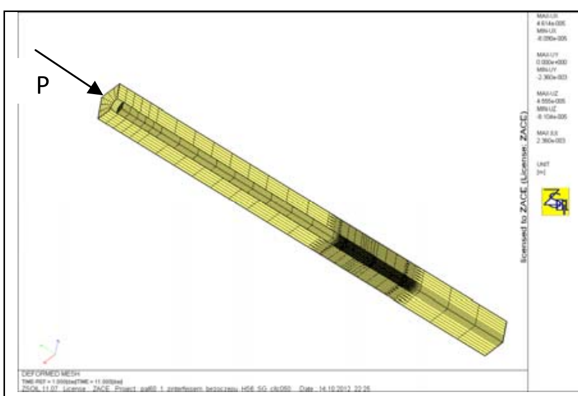

a) Deformed FE mesh, 1/4 of periodic cell, D=0.6m, |umax|=$2.36\cdot10^{-3}$m at the top of pile

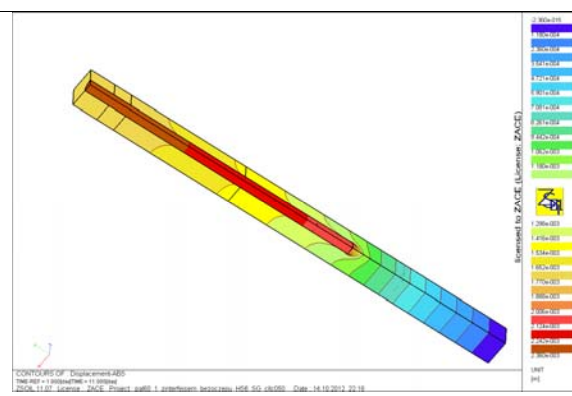

b) Map of |u| for P=1000kN , |umax|=$2.36\cdot10^{-3}$m at the top of pile

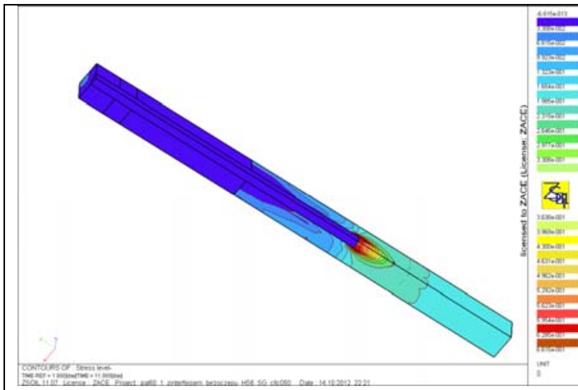

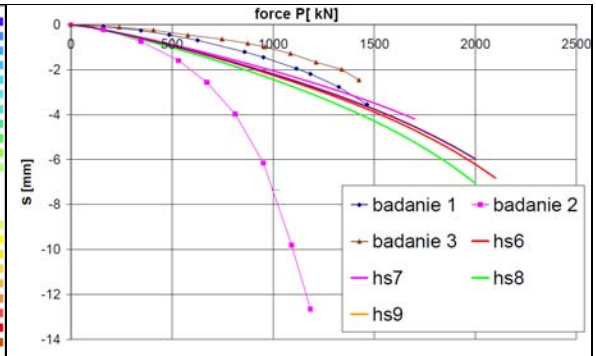

d) Load-displacement curves

c) Map of the stress level (0<SL<1) for P=1000kN SL=0.6615 at the pile tip

-measured for different piles (marked lines)
-simulated for different sets of HS-s model data (smooth lines)

Fig.4.2 Results of back analysis concerning single D=0.6m pile

Selected results for the 2 groups of micro-piles (D=0.2m), i.e. 3x3 and 3x5 are presented in Fig 4.3.

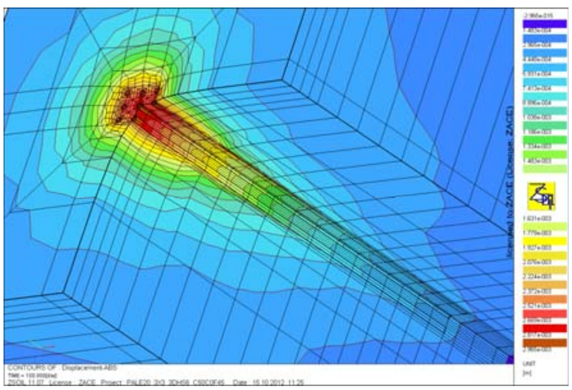

a) Deformed FE mesh of 3x3 D=0.2m pile system, map of |u|, $|u_{max}|=2.96\cdot10^{-3}$m at the top of the central pile

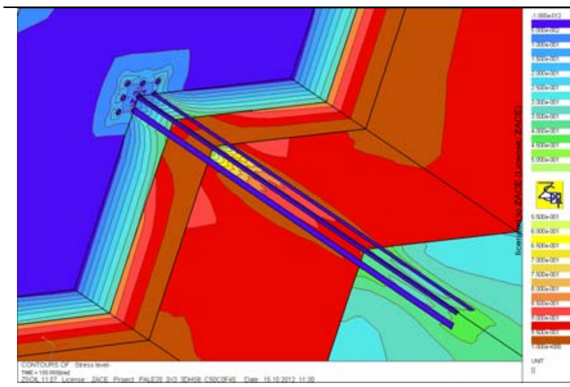

b) Map of the stress level for 3x3 (0<SL<1)

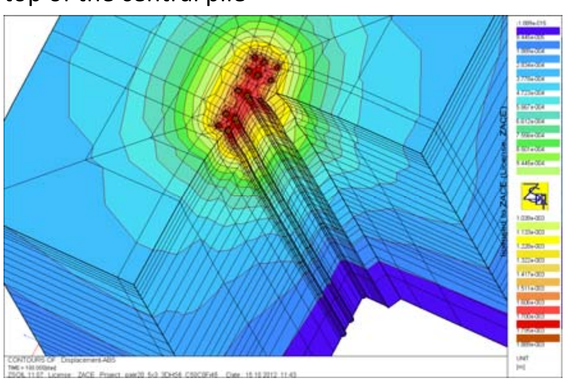

c) Deformed FE mesh of 3x5 D=0.2m pile system, map of |u|, $|u_{max}|=1.889\cdot10^{-3}$m at the top of the central pile

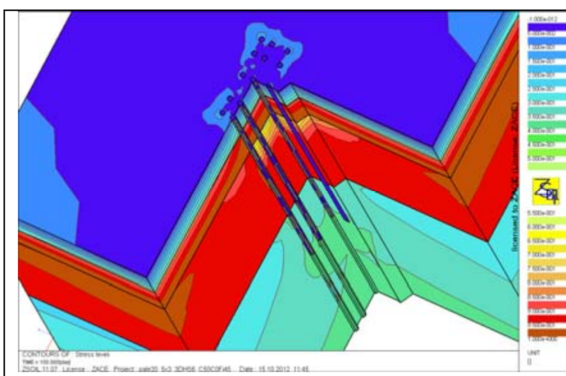

d) Map of the stress level for 3x5 (0<SL<1)

Fig.4.3 Results of simulation of D=0.2 pile groups

It is worth mentioning , that for both groups an artificial foundation is created at the bottom of the piles. Moreover, displacement-load relations remain quasi-linear, in the considered load range.

Results of predictions shown in Fig. 4.2 and Fig 4.3 were obtained using real 3D model in which subsoil and pile are discretized using continuum brick elements without simplifications described in section 2. This kind of approach is always possible, but in a practice it is time consuming as the resulting 3D mesh is usually very large (in the paper only a single pile or relatively small group of piles were analyzed, but problems arise with larger number of piles). To compare these two ways of modeling a group of 3x3 micro-piles, loaded up to $\Sigma P=9x250=2250kN$ (which in the considered case was maximal design load) , is analyzed. The analyzed models are shown in Fig.4.4.

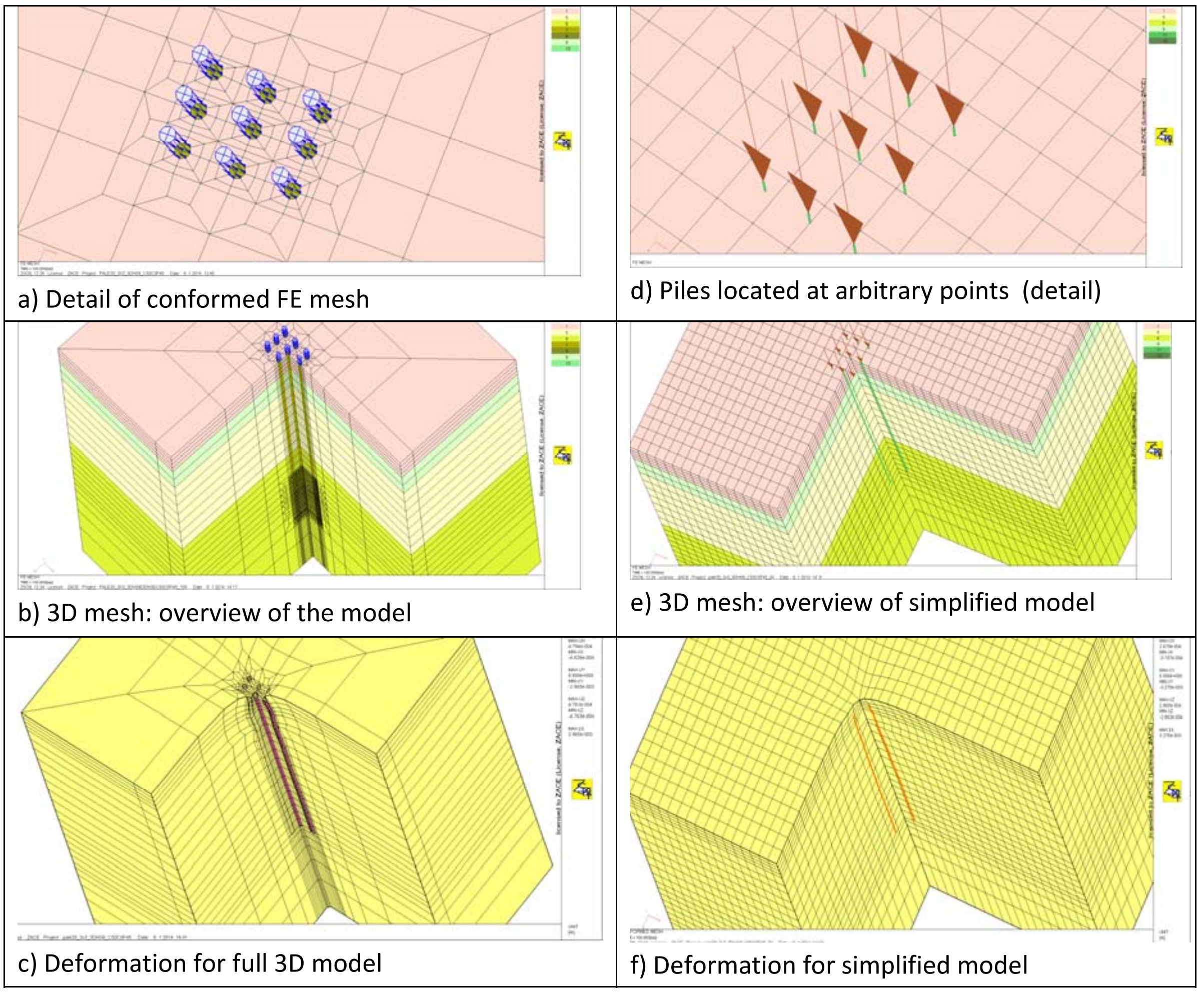

a) Detail of conformed FE mesh

d) Piles located at arbitrary points (detail)

b) 3D mesh: overview of the model

e) 3D mesh: overview of simplified model

c) Deformation for full 3D model

f) Deformation for simplified model

Fig.4.4 a), b), c) FE mesh for full 3D model. d), e) , f) Simplified model of piles with regular FE mesh

Deformation pattern for both models agree qualitatively (see Fig.4.4c 4.4.f)). Quantitatively, simplified model yields slightly stiffer response, for the maximum displacement $Uy_{Simpl}=2.5mm$, while $Uy=3mm$ for conformed FE mesh.

5. Summary and conclusions

The two alternative approaches for modeling micropile-subsoil interaction have been shown in the paper. The most general approach in which each micropile is discretized with 3D elements and the interface is a real surface is too complicated and time consuming at the early stage of design of complex foundations enhanced by micropiles or piles. Therefore a simplified approach in which micropiles are discretized using beam elements embedded through the special Coulomb's interface in the 3D continuum is beneficial. In the latter case any modification of the micropile system does not affect the existing 3D model of foundation and subsoil. In both cases the simplest method of taking into account the effect of micropile installation can be realized by using the *K* pressure method proposed in report [7] that locally modifies stress state around the micropile by increasing radial stresses. This procedure is not yet fully automatic for the simplified approach and is currently in stage of development.

Literature

1. Benz T. (2006). Small-strain stiffness of soils and its numerical consequences. Phd, Universitat Stuttgart

2. A. Truty, K. Podleś. Modele MES wielko-gabarytowych płyt fundamentowych wzmacnianych układem pali. Czasopismo Techniczne (Technical Transactions) 2009.

3. R. Obrzud, A. Truty. The Hardening Soil model- a practical guidebook. Z Soil.PC 100701 report revised 31.01.2013. ZACE Servicesz Ltd. 2010.

4. O.C. Zienkiewicz R.L. Taylor. The Finite Element Method. Fourth edition. McGraw-Hill Book Company (UK) Limited. 1989.

5. ZSOIL 2013. User manual. Elmepress International, Lausanne.

6. PN-83-B-02482: Fundamenty Budowlane Nośność Pali i Fundamentów Palowych.

7. Syawal Satibi, Ayman Abed, Chuang Yu, Martino leoni and Pieter A. Vermeer. FE simulation of installation and loading of a Tube-Installed Pile. 2007. Institutsbericht 29 des Instituts fűr Geotechnik Herausgeber P.A. Vermeer.